Preparation and electrochemical properties of PPy/$LiCoO_2$ composites cathode materials for lithium battery

KARIMA FERCHICHI[a], SEIF EDDINE BOUGHDIRI[a], NOUREDDINE AMDOUNI[a*], VALERIE PRALONG[b]

[a]*UR Physico-Chimie des Matériaux condensés, Faculté des Sciences de Tunis, Manar II, 2092 Tunis, Tunisia.*
[b] *Laboratoire de cristallographie et sciences des matériaux CRISMAT ENSICAEN, 6 Bd Marechal Juin, 14050 Caen, France.*

(Reçu le 28 Avril 2014, accepté le 15 Octobre 2014)

ABSTRACT: Layered $LiCoO_2$ was synthesized by sol-gel process, and a polypyrrole/ $LiCoO_2$ composite was then prepared by polymerizing pyrrole monomer in Pickering emulsion stabilized by $LiCoO_2$ particles. The bare sample and composite were subjected to analysis and characterization by the techniques of X-Ray Scattering (*WAXS*), infrared spectroscopy (IR) and scanning electron microscopy (SEM). The electrochemical properties of the composite were investigated with galvanostatic charge-discharge test and, which shows that the polypyrrole (PPy) significantly decrease the charge-transfer resistance $LiCoO_2$. The composite containing 25 wt% PPy exhibits a good electrochemical performance, its specific discharge capacity is 178 $mAhg^{-1}$ at C/20 rate and voltage limits of 3-4.5 V, while the capacity of the bare sample is only 136 $mAhg^{-1}$.

Keywords: PPy; Conducting Polymer; composite materials; lithium battery.

1. INTRODUCTION

Lithium transition metal oxides, such as $LiCoO_2$, $LiNiO_2$, $LiMn_2O_4$, have been extensively studied as cathodes of the secondary lithium batteries due to their high output voltage and high specific energy [1]. Among these oxides, $LiCoO_2$ has been used as cathode since 1990 [2] and it is still considered a material with favorable electrochemical performance properties despite its cobalt-related high cost [3]. Layered $LiCoO_2$ is usually cycled to an upper cutoff voltage of 4.2 V versus Li and gives a specific capacity of 140 $mAhg^{-1}$. However, its high cost and toxicity limit its further use in newly developed multifunctional portable devices and electric vehicle systems [2].

In recent years, conducting polymers, such as polypyrrole (PPy), polyaniline (PANI), and poly (3,4-ethylenedioxythiophene) (PEDOT), have been attracting much attention as additives or coating materials for lithium ion batteries. PPy has been known as an inherent electrical conductive polymer due to the conjugation of the single and double bonds alternating within the macromolecular architecture. The extra electrons of the double bond in a conjugated system are free to move or roam through the polymer chain, which induces electrical conductivity. PPy was also found to be electrochemically active for lithium ion insertion and extraction in the voltage range of 2.0–4.5V versus Li/Li^+, with a theoretical capacity of 72 $mAhg^{-1}$. Therefore, PPy additives can be used as both conductive agents and cathode materials [4]. Investigations on CVO/PPy [5], $LiMn_2O_4$/PPy [6], LiV_3O_8/PPy [7], $Co_{0.2}CrO_x$/PPy [8], and $LiFePO_4$/PPy [9] have been reported. Pasquier et *al*. [10] have coated $LiMn_2O_4$ particles with PPy to improve the cyclability of $LiMn_2O_4$ cathode at elevated temperatures by suppressing the dissolution of Mn in the $LiPF_6$ electrolyte.

In this paper, we attempt to incorporate polypyrrole into $LiCoO_2$ using the chemical oxidation polymerization method and to prepare a novel organic–inorganic composite, PPy/$LiCoO_2$, with the aim of improving the electrochemical performance of $LiCoO_2$ cathode. The structure, morphology and electrochemical properties of PPy/$LiCoO_2$ were systematically investigated. Preliminary

* Corresponding author, email : nouredin.amdouni@fst.rnu.tn

experiments showed that the incorporation of PPy onto $LiCoO_2$ resulted in higher specific capacity over bare $LiCoO_2$ material.

2. MATERIALS AND METHODS

2.1. Materials and methods

Pyrrole monomer (Across) was purified by vacuum distillation and was stored in refrigerator before use. Ammonium persulfate ($(NH_4)_2S_2O_8$, APS, Across) was used as an oxidant. Hydrochloric acid (SIGMA-ALDRICH) and toluene (SIGMA-ALDRICH) were used as received without further purification. Lithium acetate (SIGMA-ALDRICH), cobalt acetate (SIGMA-ALDRICH) and citric acid (SIGMA-ALDRICH) were used to prepare $LiCoO_2$.

2.2. Synthesis of $LiCoO_2$

The $LiCoO_2$ particles were synthesized by the sol-gel process based on citric acid [10]. Stoichiometric amounts of $Li(CH_3COO).2H_2O$ and $Co(CH_3COO)_2.4H_2O$ were dissolved in deionized water; aqueous citric acid solution was added to this solution at 80°C while stirring until a gel formed. The resulting gel was dried at 120°C for 12 h in air to extract out excess water, yielding a dry puffy precursor. The gel precursor was preheated at 500°C for 24 h in air in order to decompose organic materials and calcination was thereafter performed at 750°C for 24 h to yield the final $LiCoO_2$ product.

2.3. Synthesis of PPy/$LiCoO_2$ composite materials

The PPy/$LiCoO_2$ composite materials were prepared in a $LiCoO_2$ nanoparticle stabilized Pickering emulsion. To prepare the Pickering emulsion, the $LiCoO_2$ was first dispersed in water using an ultrasonic disperser Sonics VibraCell equipped with a 25 mm shaft working at 20 kHz, 500W power and 80% of the full amplitude (Bioblock Scientific, France). The oil phase solutions consisting of pyrrole dissolved in toluene. The oil and aqueous phases were mixed with an ultrasound disperser Sonics VibraCell at 500W during 2 min, emulsions were prepared with 25 wt.% of pyrrole. Then pH value of the Pickering emulsion was adjusted to 4 using 1 M HCl solution. Polymerization was carried under agitation in cold bath (0 to 5 °C) by slow addition of a solution of ammonium persulfate (APS). The precipitated PPy/$LiCoO_2$ material was collected by Centrifugation using a Beckman-Coulter Optima™ MAX-E ultracentrifuge equipped with a MLA-80 rotor thermostated at 30000 rpm for 30 min at 20 °C. Then the precipitate was washed with water and ethanol to remove salts and organic impurities. The recovered fine powder was dried under vacuum at 50 °C and kept in desiccators until used. PPy was prepared by *in situ* polymerization of pyrrole using ammonium persulphate $(NH_4)_2S_2O_8$ as an oxidant in acidic medium in the presence of HCl (0.1 M) solution.

2.4. Methods

Infrared spectra of the various samples and thin films pressed as KBr pellets were recorded in transmission mode with a Perkin Elmer 1000 spectrometer in the range 400-2000 cm^{-1}. Wide Angle X-Ray Scattering (*WAXS*) of powder samples were performed using a Philips X'pert diffractometer working with the Cu$K\alpha$ line (λ = 1.5451 Å). Scanning electron microscopy (SEM) images were obtained using a Philips Field Effect Gun (FEG) XL-30, at an accelerating voltage of 5 kV without sample metallization.

Electrochemical measurements were conducted in Li/$LiPF_6$ (PC/EC)/(PPy/$LiCoO_2$). The positive electrode was prepared as pellets of 0.8 cm diameter using 1 g of either the composite or the pristine oxide mixed with 20 wt.% acetylene black (Denka Singapore Pvt. Ltd.) and with 5 wt.% PVDF pressed at 3 tcm^{-2} and heated at 60 °C for 12 h. The cells, assembled into an argon-filled dry box (mBraun, 120G, and Germany) in Swagelok type cells. Teklon (Anatek, USA) was used as the separator and lithium metal (Aldrich, 99.9 %) as counter electrode. A borosilicate glass fiber sheet saturated with electrolyte used as the separator. The electrolyte was 1 M $LiPF_6$ in a mixed (1:1) solvents of ethylene carbonate (EC) and dimethyl carbonate (Chile Industries Ltd., Korea). Electrochemical experiments were carried out using the BIO-LOGIC SA multichannel model VMP2, at room temperature (25°C). The cells were galvanostatically tested in the range of 3–4.5 V to evaluate the electrochemical behavior of the cathode materials.

3. RESULTS AND DISCUSSION

3.1.1. Nature of the inorganic phase from WAXS

The Rietveld refinement of XRD patterns of $LiCoO_2$ was presented in Figure 1. The diffraction pattern of $LiCoO_2$ displayed sharp Bragg reflexions that were indexed to a hexagonal lattice layered rhombohedral structure with a well-established $R\bar{3}m$ space group, in agreement with previous reports in the literature [11]. The higher intensity ratio of the (006)/(102) and (108)/(110) diffraction peaks, together with the clear splitting of the (003) and (104) diffraction peaks, confirmed the layered nature of the material [12]. The crystallographic parameters for the $LiCoO_2$ are found to be a = 2.815 Å and c = 14.056 Å. The coherent domain size (CDS) was determined by measuring the broadening of the diffraction lines using the whole pattern analysis Rietveld method. The CDS of $LiCoO_2$ was around 65 nm.

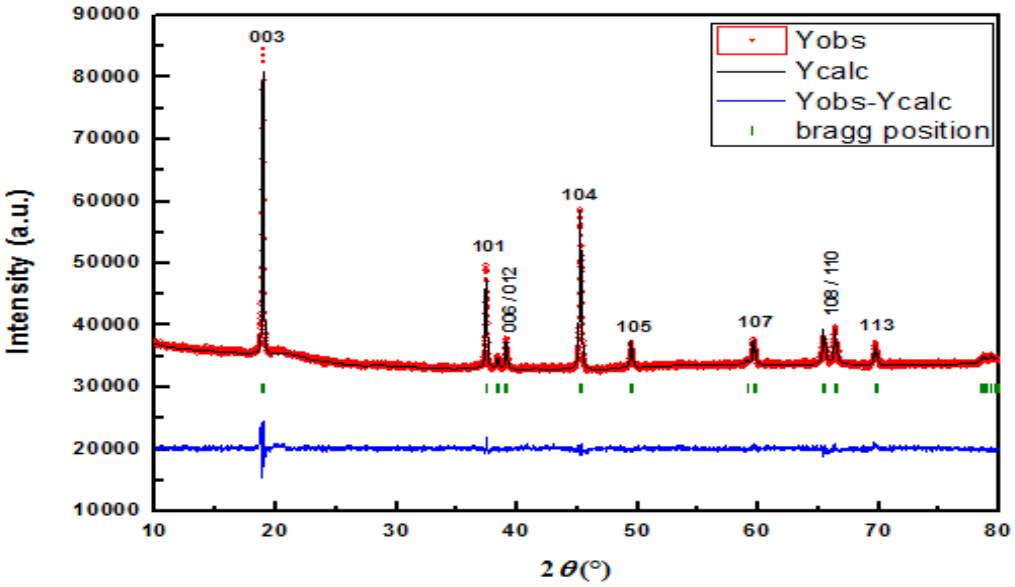

Figure 1 : Rietveld refinement of XRD patterns of $LiCoO_2$ using the hexagonal $R\bar{3}m$ symmetry.

Figure 2 shows the XRD pattern of the synthesized PPy, $LiCoO_2$ and PPy/$LiCoO_2$ composite material. The XRD pattern of PPy is in good agreement with the reported literature [13]. X-ray diffraction studies show that the PPy powder is amorphous in nature, as shown in Figure 2. Broad peak was observed at about 2θ = 26°, This peak is characteristic of amorphous PPy [14] and are due to the scattering from PPy chains at the interplanar spacing [15]. The average chain separation can be calculated from these maxima using the relation [16].

$$S = 5\lambda / 8\sin\theta \qquad (1)$$

Where S is the polymer chain separation, λ is the X-ray wavelength and θ is the diffraction angle at the maximum intensity of the amorphous halo. The average chain separation was found to be 4.30 Å for PPy. The average crystallite size from a sharp peak at 26° for PPy is estimated by using the Scherrer's formula [17].

$$D = K\lambda / \beta\cos\theta \qquad (2)$$

Where D is the crystallite size, K is the shape factor, which can be assigned a value of 0.89 if the shape is unknown, θ is the diffraction angle at maximum peak intensity, and β is the full width at half maximum of diffraction angle in radians. When applied to the sharp peaks, Equation (2) leads to the average crystallite size of about 46 nm for PPy powder.

The Rietveld refinements of XRD patterns of $LiCoO_2$ and PPy/$LiCoO_2$ composite material were performed using the hexagonal $R\bar{3}m$ symmetry. The refined lattice and coherent domain sizes are given in Table I. Compared with pristine $LiCoO_2$, the values a, c, and v of PPy/$LiCoO_2$ composite material decrease due to PPy effect on the crystal structures. The composite CDS was 62 nm.

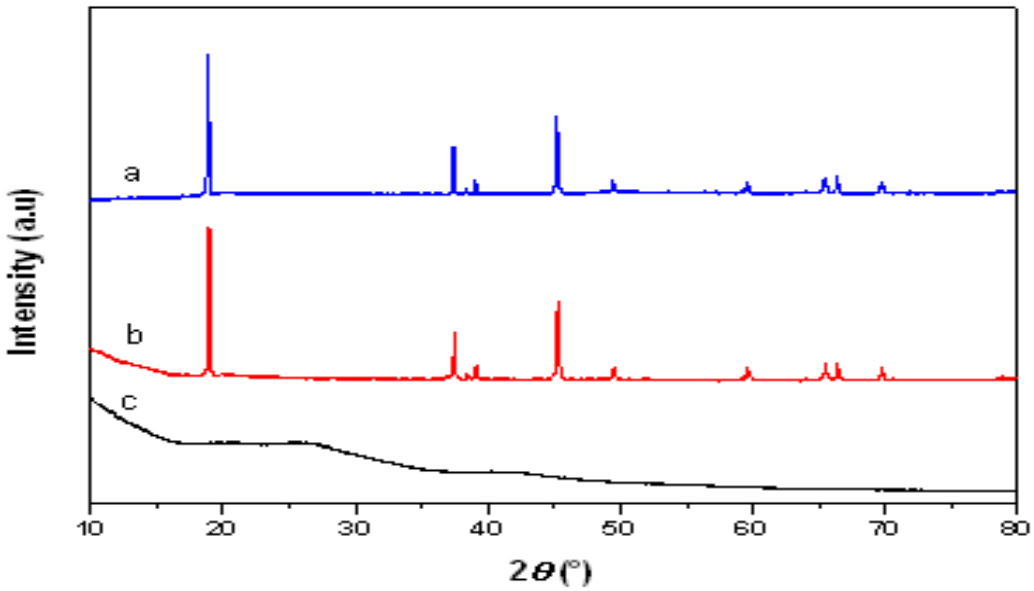

Figure 2 WAXS patterns of PPy, $LiCoO_2$, and PPy/$LiCoO_2$ composite material.

Table I : The structural parameters of $LiCoO_2$ and PPy/$LiCoO_2$ composite material

	$LiCoO_2$	**PPy/$LiCoO_2$**
***a* (Å)**	2.815	2.814
***c* (Å)**	14.056	14.052
***v* (Å^3)**	96.462	96.432
I_{003}/I_{104}	1.907	1.662
CDS (nm)	65.636	62.953

3.1.2. IR spectroscopy

Figure 3 shows the FT–IR spectrum of PPy, $LiCoO_2$ and PPy/$LiCoO_2$ composite material. The characteristic bands of PPy can be observed at 1552–1699 cm^{-1} (C=C stretching vibration of doped PPy ring), 1471 cm^{-1} (C–N stretching mode of doped PPy), 1303 cm^{-1} (C–H or C–N inplane deformation modes). Admixing of PPy with $LiCoO_2$ cathode would reduce the particle-to-particle separation and also resistance which significantly enhances the electrical conductivity of the composites [18]. All bands shifted to higher wave numbers in the composite material PPy/$LiCoO_2$ (Table II), which indicated that some interaction existed between PPy and $LiCoO_2$ particles [19]. The absorption band at 600 cm^{-1} represents the vibration on octahedral CoO_6 while the vibration at 555 cm^{-1} can be attributed to the tetrahedral LiO_4 [20].

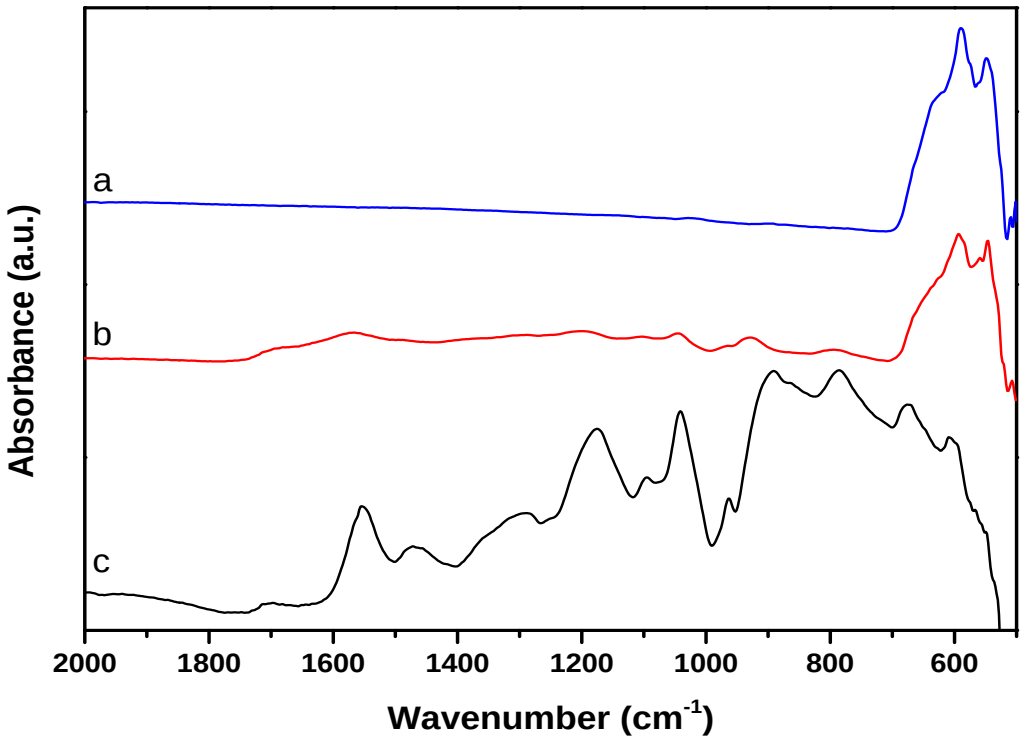

Figure 3 : IR spectra of PPy, $LiCoO_2$, and PPyI/$LiCoO_2$ composite material.

Table II : Assignments of the main peaks in the IR spectra of PPy and PPy/$LiCoO_2$ composite material

Peak assignments (wave numbers in cm^{-1})	PPy	PPy/$LiCoO_2$
N-H wagging	786	800
N-H wagging	1043	1045
C=N stretching	1178	1198
Mixed bending and stretching vibrations associated with C-N links	1303	1303
C-C, C-N stretching	1471	1489
C=C stretching	1552	1569

3.2. Scanning electron microscopy

Evidence of the presence of inorganic and organic phases in the hybrid composite materials has been given by WAXS and IR analyzes. The morphology of the organic/inorganic alloys affects the material transfer phenomena and the electrical properties through the lithium exchange processes that come along with the oxidation/reduction of cobalt in the Li-batteries. The structure and morphology of the PPy/$LiCoO_2$ material was characterized by scanning electron microscopy. Scanning emission scanning electron microscopy pictures of the PPy, $LiCoO_2$ and PPy/$LiCoO_2$ composites hybrid structures are shown in Figure 5. SEM of PPy exhibited a nanospherical-like morphology with particle diameter around 0.30 µm. The morphology of $LiCoO_2$ was characterized by the agglomerates of elementary thin platelets; the agglomerates observed by SEM had the shape of porous particles with a well-defined round shape. The SEM image of 25 wt.% PPy/$LiCoO_2$ composite show that the particles of $LiCoO_2$ are encapsulated in the matrix of polypyrrole, which are formed uniformly over the surfaces of the $LiCoO_2$ particles. The coating of conducting PPy on

the surface of $LiCoO_2$ crystals can reduce the particle-to-particle contact resistance and improves the conductivity of the composite.

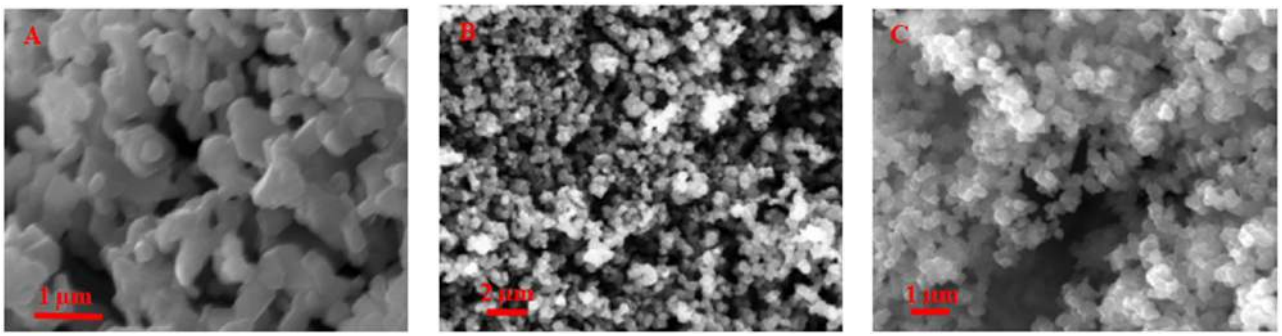

Figure : 5 SEM of (A) $LiCoO_2$, (B) PPy, and (C) PPy/$LiCoO_2$ composite material.

3.3. Electrochemical performance

The electrical properties of $LiCoO_2$ and PPy/$LiCoO_2$ composite were assessed at room temperature by electrochemical measurements were conducted in Li/$LiPF_6$ (PC:EC)/(PPy/$LiCoO_2$). The charge-discharge curves of $LiCoO_2$ and PPy/$LiCoO_2$ composite used as positive electrodes for rechargeable lithium batteries at room temperature with C/20 rate in the range of 3-4.5 V are shown in Figure 6. The charge and discharge capacities of $LiCoO_2$ were 189 and 136 $mAhg^{-1}$, respectively, showing a 72% coulombic efficiency. The obtained values were in good agreement with the results reported by other authors [21, 22]. The PPy/$LiCoO_2$ composite material has shown a good electrochemical performance. The PPy/$LiCoO_2$ composite material shows a higher discharge capacity than that of $LiCoO_2$ which works better as an electrode for lithium insertion–deinsertion compared to the pristine $LiCoO_2$.This electrochemical behaviour was in agreement with the results reported in the literature [6, 8] for composite materials using PPy as organic compound. The charge and discharge capacities of PPy/$LiCoO_2$ composite were 189 and 178 $mAhg^{-1}$, showing a 94% coulombic efficiency. These values were higher than those reported in literature for other composite materials such PPy/$LiFePO_4$ and PPy/$LiMn_2O_4$ [9, 6] and similar to those reported for PPy/ $LiNi_{1/3}Mn_{1/3}Co_{1/3}O_2$ [23].

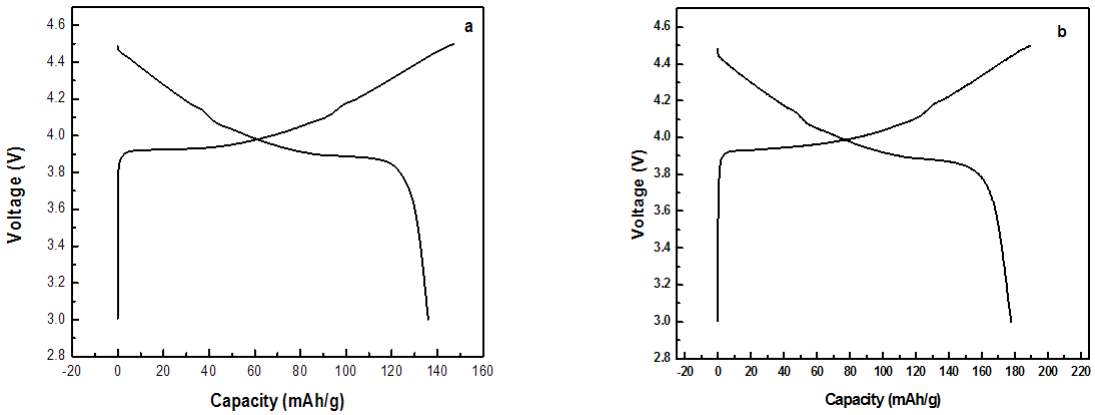

Figure 6 : First charge-discharge profile of (a) $LiCoO_2$ and (b) PPy/$LiCoO_2$ composite material cell at the rate C/20 in the voltage window (3–4.5 V).

The discharge capacity of $LiCoO_2$ and PPy/$LiCoO_2$ composite material at different C rates in the range of 3-4.5 V showed that C/20 was the perfect rate (Figure 7).

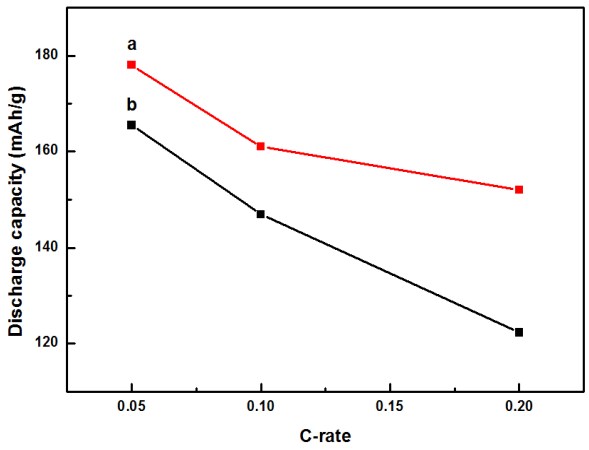

Figure 7 : Evolution of the capacity as a function of the discharge C-rate for for (a) PPy/$LiCoO_2$ composite material and (b) $LiCoO_2$.

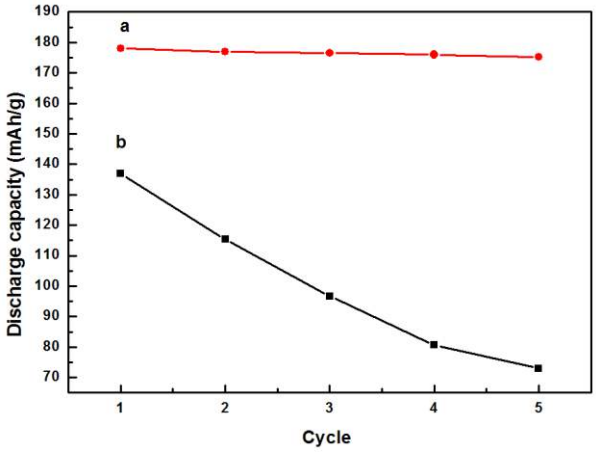

Figure 8 : Evolution of the capacity as a function of the cycling life at C/20 rate for (a) PPy/$LiCoO_2$ composite material and (b) $LiCoO_2$.

The cycling abilities of $LiCoO_2$ and PPy/$LiCoO_2$ composite material were examined via galvanostatic cycling test (Figure 8). PPy$LiCoO_2$ was demonstrated the best cycling performance during 5 cycles showing discharge capacity and coulombic efficiency about 178 $mAhg^{-1}$ and 94% respectively and remains at 175 $mAhg^{-1}$ after 5 cycles, which is 98% of the initial capacity. The stability is due to the PPy that makes a stable structure during the Li insertion-extraction reaction, the electrical conductivity can be significantly improved which facilitates the charge-transfer reaction, leading to better utilization of the active materials.

4. CONCLUSIONS

The PPy/$LiCoO_2$ composite material was prepared by polymerization of pyrrole monomer in Pickering emulsion stabilized by $LiCoO_2$ particles. The evaluating the electrochemical performance of PPy/$LiCoO_2$ composite material confirmed that the PPy improved the electrochemical properties of $LiCoO_2$ and therefore facilitated the charge-transfer reaction. This composite maintains the Li-insertion ability of the $LiCoO_2$ counterpart and shows improved behavior as an electrode for rechargeable lithium batteries. The enhanced electrochemical performance of the composite may result from the decrease of the charge transfer resistance.

References

[1] E.I. Santiago, A.V.C. Andrade, C.O. Paiva-Santos, L.O.S. Bulhoẽs, *Solid State Ionics*, **2003,** *158*, 91.
[2] K. Brandt, *Solid State Ionics*, **1994,** *69*, 173.
[3] R. Koksbang, J. Barker, H. Shi, M.Y. Saïdi, *Solid State Ionics*, **1996**, *84*, 1.
[4] G.X. Wang, L. Yang, Y. Chen, S. Bewlay, H.K. Liu, *Electrochim. Acta*., **2005,** *50*, 4649.
[5] S. Zhang, Y. Sun, C. Li, R. Hu, *Mater. Lett.*, **2013,** *91***,** 154.
[6] J.U. Kim, I.S. Jeong, S.I. Moon, H.B. Gu, *J. Power Sources*, **2001**, 97-98, 450.
[7] S.Y. Chew, C. Feng, S.H. Ng, J. Wang, Z. Guo, H. Liu, *J. Electrochem. Soc*., **2007**, *154*(7), A6330.
[8] R.P. Ramasamy, B. Veeraraghavan, B. Haran, B.N. Popov, *J. Power Sources*, **2003**, *124*, 197.
[9] G.X. Wang, L. Yang, Y. Chen, J.Z. Wang, Steve Bewlay, H.K. Liu, *Electrochimica Acta*., **2005**, *50*, 4649.
[10] A.D. Pasquier, F. Orsini, A.S. Gozdz, J.M. Tarascon, *J Power Sources*, **1999**, *81*, 607.
[11] J.N. Reimers, J.R. Dahn, *J. Electochem. Soc*., **1992**, *139*, 2091.
[12] S. Neves, S.C. Canobre, R.S. Oliveira, C. P. Fonseca, *J Power Sources*, **2009**,*189*, 1167.
[13] M.A. Chougule, S.G. Pawar, P.R. Godse, R.N. Mulik, S. Sen, V.B. Patil, *Soft Nanoscience Letters*, **2011**, *1*, 6.
[14] R.E. Partch, S G. Gangoli, E. Matijevic, W. Cai, S. Arajs, *J. Colloid and Interf. Sci.*, **1991**, *144*, 27.
[15] J. Y. Ouyang, Y.F. Li, *Polymer*, **1997**, *38*, 3997.
[16] K. Cheah, M. Forsyth, V.T. Truong, *Synthetic Met.*, **1998**, *94*, 215.
[17] B. D. Cullity, Elements of X-Ray Diffraction, Addison-Wesley Publishing Company Inc., London, 1978.

[18] R.B. Shivashankaraiah, H. Manjunatha, K.C. Mahesh, G.S. Suresh, T.V. Venkatesha, *J. Solid. State Electrochem*., DOI 10.1007/s10008-011-1520-7.
[19] G.P. Song, J. Bo, R. Guo, *Colloid Polym. Sci.,* **2005,** *283*, 677.
[20] L. Predoană, A. Barău, M. Zaharescu, H. Vasilchina, N. Velinova, B. Banov, A. Momchilov, Proceedings of the International Workshop "Advanced Techniques for Energy Sources Investigation and Testing" 4–9 Sept Sofia, Bulgaria, **2004**.
[21] D.H. Kim, E.D. Jeong, S.P. Kim, Y.B. Shim, *Bull. Korean Chem. Soc*., **2000**, 21, 1125.
[22] K. Teshima, S. Lee, Y. Mizuno, H. Inagaki, M. Hozumi, K. Kohama, K. Yubuta, T. Shishido, S. Oishi, *J. Am. Chem. Soc*., **2010**, doi:10.1021/cg100705d.
[23] P. Zhang, L. Zhang, X. Ren, Q. Yuan, J. Liu, Q. Zhang, *Synthetic Met.,* **2011**, *161*, 1092.